

Effect of Irradiation on Electrical Conduction and Crystallization in Ge_{1-x}Si_x Films

Heydar Mahdavi and Rahim Madatov

Institute of Radiation Problems, Azerbaijan National Academy of Sciences, Baku, Azerbaijan

*E-mail: mahdavi1382@yahoo.com

Received: 29 October 2013 / Accepted: 4 December 2013 / Published: 5 January 2014

Influence of thermal annealing and effect of gamma irradiation on electrical conduction in Ge_{1-x}Si_x ($0 \leq x \leq 15$) films were studied. The films were deposited from molecular beams in ultrahigh vacuum. The influence of thermal annealing and the effect of gamma irradiation were investigated by the X-ray diffraction analysis and the electric conductivity method. It was found that the thermal annealing of amorphous Ge_{1-x}Si_x films increases their resistivity due to fractional crystallization in the films. The irradiation of the samples by an electron beam with an energy of 1.26 MeV and a dose of 10^{16} cm⁻² increases the crystallization temperature from 460 up to 560 K (with an increase of the Si content in Ge).

Keywords: germanium–silicon alloys, epitaxial film, electrophysical properties, heterostructure

1. INTRODUCTION

Silicon-based materials are of great interest because of wide use in solar power system and of great progress in silicon technology. The photodetectors based on Si/Ge quantum wells with a photosensitivity in the 6-20 μm range are alternative to the photodetectors based on the A₂B₆ compounds [1-3]. Ge and Si have unlimited mutual solubility in the liquid and solid states, and this agrees well with the nature of these elements. They are similar in chemical properties. They have similar atomic radii and occupy adjacent places in the electrochemical series. Ge and Si have the diamond-type lattice. The ratio $a_{\text{Ge}}/a_{\text{Si}}=1.042$, i.e. the difference of lattice parameters is less than 4.3% [4].

Authors of the phase diagram [5] noted that under normal conditions the alloy crystallization is nonuniform. With a decrease in temperature, the concentration of solid phase, precipitated under cooling, remains increased as compared with equilibrium one. The phase diagram was studied

theoretically and it was shown that for correlation between theoretical and experimentally observed solidus and liquids curves, it is necessary to accept that the interaction between identical atoms (Ge–Ge and Si–Si) should be weaker than between Ge–Si atoms, so there is an ordering tendency in the solid solution.

The results of work [6] have shown that the number of interstitial atoms in the Ge–Si solid solution is so small that it is beyond the sensitivity threshold of X-ray analysis. According to the X-ray data, the lattice constant of Ge–Si alloys changes linearly with the composition. The Si atoms deform the Ge lattice and decrease its parameter.

2. MATERIALS AND METHODS

In the $\text{Ge}_{1-x}\text{Si}_x$ ($0 \leq x \leq 15$) alloy, the Ge and Si atoms are placed randomly in the diamond-type lattice sites. Since the alloy is not a perfect crystal, there is a disturbance of lattice periodicity. Therefore, the alloy does not have an energy band structure in a strict sense, but one can suggest some features of energy band structure in the alloy.

Electron energy spectrum consists of a large number of energy intervals with high density of states. The alloy energy spectrum consists of a large number of energy intervals with low density of states: they are forbidden bands mainly. One can consider that the alloy energy spectrum consists of a large number of bands with high density of states which have small “tails” (regions with low density of states) penetrating into the forbidden bands (regions with negligibly small density of states). Since the difference of lattice parameters in Ge and Si is less than a few percent, and their atoms are of the same valence, it is most likely that the “tails” in the energy spectrum of $\text{Ge}_{1-x}\text{Si}_x$ alloy are rather of secondary (not of primary) importance.

Much attention was given to the investigation of electrical properties of the heavily doped and compensated solid solution [4]. It was established that in the 300–700 K range the mobility decreases with temperature as $T^{-1.1}$ and $T^{-0.9}$ for the noncompensated and compensated samples, respectively [4]. From these data, the ion contribution to the mobility was determined [5]. For scattering by structural irregularity $\mu \sim T^{-0.8}$. For lattice-vibration scattering $\mu_r \sim T^{-3.5}$, and in the 50–100 K range $\mu_r \sim T^{-2}$ [6]. In the $\text{Ge}_{1-x}\text{Si}_x$ solid solutions with the Si content up to 15%, the hole mobility for lattice-vibration scattering in the 100–280 K range changes as $\mu_p \sim T^{-2.33}$, just like in pure Ge [7].

To perform the process of vacuum evaporation of the substance, one needs an evaporator that can contain the evaporated substance and maintain its temperature at a level sufficient for necessary vapor pressure. The deposition rate of the films can vary from values less than 1 Å/s to values greater than 1000 Å/s.

The operating temperature of the evaporator can be estimated from the condition that a steady-state vapor pressure of the evaporated material (the Ge–Si solid solution) on the order of 10^{-2} mm Hg is needed to provide a rate of the film deposition on the order of 4.5–5 nm/s. Tungsten was used as a material for the evaporator (its temperature was maintained at 2100 K). The evaporator in the form of a boat 4 cm long and 1 cm wide was made in the laboratory. The only problem that we experienced while making the evaporator was caused by the tungsten brittleness. The ends of the electric contacts

were connected to the copper contact terminals.

The condensation of a molecular beam with some density (the number of atoms that reach the substrate in a unit of time) occurs only at a temperature that does not exceed some critical temperature T_{cr} . The critical flux density is always present, and at the specific temperature T_{cr} the condensation on the given substrate begins [8]. There is an idea that the migration of the adsorbed particles on the substrate surface is isotropic process. This idea is true for amorphous substrates, but it should be revised for the case of condensation on a crystalline substrate.

Nucleation of vacuum condensates on a neutral (particularly, amorphous) substrate can occur according to two main mechanisms: vapor–crystal [V→C]; that is, direct condensation from the vapor state into the crystalline state occurs; and vapor–liquid [V→(L→C)]; that is, the vapor transforms into the liquid. Then the liquid can remain in the overcooled amorphous state or can crystallize [L→C].

The critical temperature was found experimentally to be $T_{cr1} \approx 2/3T_m$ (T_m is the melting temperature of the condensed material in its bulk form). Below this temperature, the mechanism V→C takes place. Over this temperature, the mechanism V→L occurs. The T_{cr1} values can vary in certain limits depending on the properties of the condensate and substrate materials, the binding energy between them, the condensation rate, and other conditions of the condensation process. Some authors [9] suggested that a second critical temperature exists: $T_{cr2} \approx 1/3T_m$. Over this temperature, the V→C mechanism takes place. Below this temperature, the mechanism V→L occurs. This assumption is based on various experimental data for a large number of condensed metals as well as some alloys. Data of microscopic and X-ray investigations and microhardness measurements give evidence that an interval ΔT_{cr} exists where heterogeneous condensation by both mechanisms (V→C and V→L) occurs. The T_{cr} and ΔT_{cr} values can vary in certain limits depending on the condensation conditions. In low-temperature range of condensation ($T_m < T_{cr}$), the deposition according to the V→L mechanism sometimes leads to the formation of metastable crystalline and amorphous (glassy) phases (V→L→C or V→L→A, where A is an amorphous phase) that completely or partly transform into more stable phases at long storage or heating [10].

When an “active” single-crystal substrate is used, there are strong bonds with the substrate, the epitaxial or autoepitaxial growth of monocrystalline layers takes place, the condensation mechanism V→L is suppressed, and the temperature range where the mechanism V→C occurs ($T_{cr1} - T_{cr2}$) widens.

The condensation mechanisms considered refer to the initial stage only. At the following stages, the nuclei of the liquid phase are not stable, and the transition into the crystalline phase (L→C) occurs. However, the preceding mechanism V→L leaves its imprint in the form of defects of the crystalline structure in the condensate. This has an effect on the structure-sensitive properties, and has been used for indirect detection of the V→L mechanism at $T_{cr2} \sim 1/3T_m$ in bulk condensates.

In modern semiconductor engineering, thermal stability of electrophysical properties is a problem of great importance. At the present time, the influence of temperature on the electrophysical properties of Ge and Si has been studied rather well, and it has been established that these two elements exhibit thermal instability when they contain oxygen. The point is that oxygen reveals both the neutral and the electrically active character in Ge and Si, and considerably changes their electrophysical properties with temperature [11]. Film condensates of the $Ge_{1-x}Si_x$ solid solutions are especially sensitive to oxidation during both the evaporation and the annealing.

3. RESULTS AND DISCUSSION

Figure 1 shows the temperature dependence of the hole mobility in the $\text{Ge}_x\text{Si}_{1-x}$ ($0 \leq x \leq 15$) crystals. As one can see from Figure 1, in crystals of the $\text{Ge}_{1-x}\text{Si}_x$ solid solutions with Si content up to 15%, for lattice-vibration scattering in the 100-280 K range, the hole mobility changes as $\mu_p \sim T^{-2,33}$, just like in pure Ge.

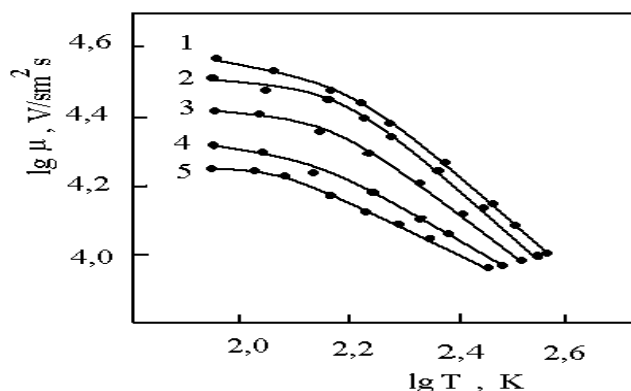


Figure 1. Temperature dependence of hole mobility in $\text{Ge}_{1-x}\text{Si}_x$ ($0 \leq x \leq 15$) crystals: (1) 0 at.%, (2) 5 at.%, (3) 10 at.%, (4) 10 at.%, (5) 15% .

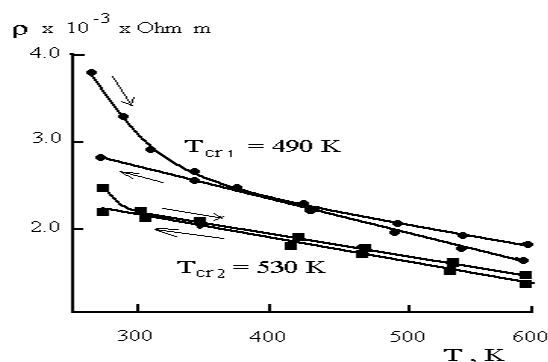


Figure 2. Temperature dependence of resistance of the $\text{Ge}_{1-x}\text{Si}_x$ ($x=0.15$) films; $n=100\text{nm}$.

A number of peculiarities associated with the behavior of conduction were found during the thermal treatment of the deposited $\text{Ge}_{0.85}\text{Si}_{0.15}$ films. The films of the $\text{Ge}_{0.85}\text{Si}_{0.15}$ solid solutions are quite resistant to thermal annealing. The condensates prepared at $T_s = 490$ K (Figure 2) were of a quasi-amorphous type. In the 350–450 K temperature range, they exhibit a semiconductor behavior of conduction with thermal activation energy of 0.052eV. This value was determined from the slope of the $\lg \sigma = f(1/T)$ dependence (Figure 3) plotted according to the experimental values. In the temperature ranges of 450–500 K and 500–680 K, the semiconductor behavior of conduction remains, but the activation energy slightly increases and makes 0.096eV. In these temperature ranges, three intervals (350–420 K, 510–540 K, and 590–620K) with more sharp change in the electrical conduction are observed. They can be associated with crystallization processes in the condensates (Fig. 4).

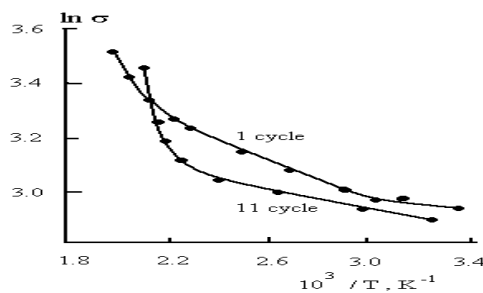


Figure 3. Dependence of conductance versus temperature in the $\text{Ge}_{1-x}\text{Si}_x$ ($x=0.15$) films at thermocycling.

As one can see from the $\lg \sigma = f(1/T)$ dependence (Figure 3), starting from 600 K the electrical conduction increases dramatically with temperature, which is caused by intrinsic conductivity. The curves 1 and 2 differ in the temperature of transition to intrinsic conductivity. At these temperatures, the activation energies are 0.22 and 0.26 eV. For the curves 1 and 2, the curve piece from 360 to 600 K corresponds to the activation energies 0.054 and 0.022 eV [12].

The crystallization kinetics and thermal stability were studied via heating the amorphous film directly in the column of UEMV-100K electron microscope using the PRON-2 attachment (Figure 4). The thermal stability of the amorphous state was determined via the appearance of the most intensive diffraction reflections of the crystalline phase against the background of the diffuse maxima of the amorphous phase. The thermal stability of the amorphous state was studied in the films deposited on the substrates at room temperature and at 490 K.

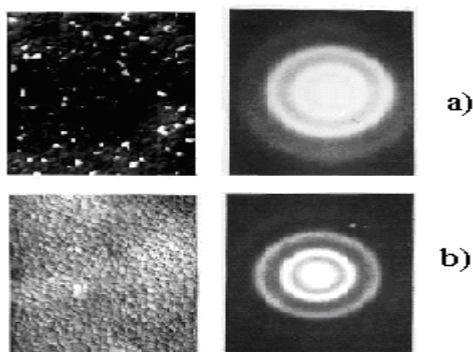


Figure 4. Micrographs and electron-diffraction patterns of the $\text{Ge}_{1-x}\text{Si}_x$ ($x=0.15$) films: $n=100\text{nm}, \times 3500$. T_s, K : (a) 490, (b) 530.

As an example, Figure 5 shows the successive stages of the structure transformations in the amorphous films. The amorphous $\text{Ge}_{0.85}\text{Si}_{0.15}$ films in initial state are not in the equilibrium, but they relax to a metastable state. When the temperature increases, the annealing of defects, changes in the free volume and in the topological short-range order occur. The composition order does not change in this process.

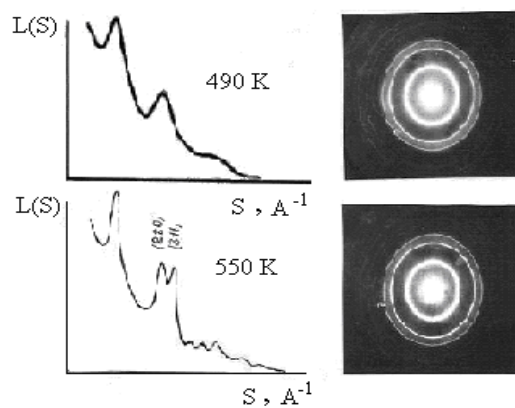


Figure 5. Crystallization kinetics of the $\text{Ge}_{1-x}\text{Si}_x$ ($x=0.15$) solid solution.

The amorphous films have a stored heat that released during the crystallization of the amorphous phase. In this process, the properties of the film change irreversibly. For practical application of the $\text{Ge}_{1-x}\text{Si}_x$ ($x=0.15$) amorphous films, it is important to know the crystallization mechanism microscopically. Such studies enable one to draw a conclusion about a possible widening of the temperature range where the amorphous films can be effectively used. The controlled crystallization can be used for making superdispersed structures [13].

The amorphous $\text{Ge}_{0.85}\text{Si}_{0.15}$ films crystallize at the temperature of 565 K. The rate of continuous heating directly in the electron microscope column is 10 K/min. Initiation of the crystallization process is registered by the appearance of the most intensive diffraction lines [(111), (220), and (311)] of the crystalline phase of the solid solution in the electron-diffraction patterns against the background of diffuse haloes. The growth of the crystalline phase occurs in a dendrite shape with formation of multiple bifurcations in the amorphous phase. When the temperature increases by 15–20 K, the crystallizations terminate with the formation of a continuous polycrystalline film of the solid solution.

The crystallization temperature of $\text{Ge}_{1-x}\text{Si}_x$ amorphous films is only 15 K greater than that of the films of amorphous Ge. This fact gives evidence that the same crystallization mechanism (diffusionless one) occurs in both cases. That is, the Si addition to Ge does not lead to a substantial increase in the thermal stability of the amorphous state. It is known that the thermal stability of the amorphous state can be considerably increased by doping with an impurity that does not form solid solutions with the host material, or has significantly different atomic radius. Hence, one should expect an increase in thermal stability of amorphous films of the $\text{Ge}_{0.85}\text{Si}_{0.15}$ system in the composition region where a decomposition of the solid solution occurs. In this case, the mechanism of the diffuse stratification of the amorphous material with the temperature rise will be a determining factor for the crystallization process. This will considerably retard the crystallization processes and lead to an increase in thermal stability of the amorphous state.

An additional crystallization at continuous heating at the rate of 25 K/min was performed to clarify the crystallization mechanism. The solution crystallization temperature is virtually the same in the case of the continuous heating with rates of 10 and 25 K/min; this proves the diffusionless behavior of interatomic restructuring in the $\text{Ge}_{0.85}\text{Si}_{0.15}$ amorphous films, as well as indicates that the interatomic

distribution in the amorphous films is highly homogeneous [14].

The irradiation of the samples by an electron beam can be performed using a defocused or focused spot (projective or objective mode of operation) at an accelerating voltage of 35 kV. The attachment allows using replaceable cutting diaphragms to vary the dimensions of the irradiated area, to measure the resistivity of the samples in the process of irradiation, and to control the temperature of the samples. The $\text{Ge}_{1-x}\text{Si}_x$ ($0 \leq x \leq 15$) samples were irradiated by an electron beam during 1.5 hours (the area of irradiated surface was 5×2 mm).

The temperature dependence of the electrical conduction in the Ge–Si samples shows that the electrical conduction decreases and the slope of the $R=f(T)$ line increases after irradiation (Figure 6); this suggests that the thermal activation energy increases. The phenomenon is most pronounced in the high-temperature region. Such a behavior of the electrical conduction in the $\text{Ge}_{1-x}\text{Si}_x$ ($x=0.15$) amorphous films indicates that the mobility gap broadens. Evidently, the action of electron flux leads to the rapid fractional crystallization and to the capture of oxygen atoms [15].

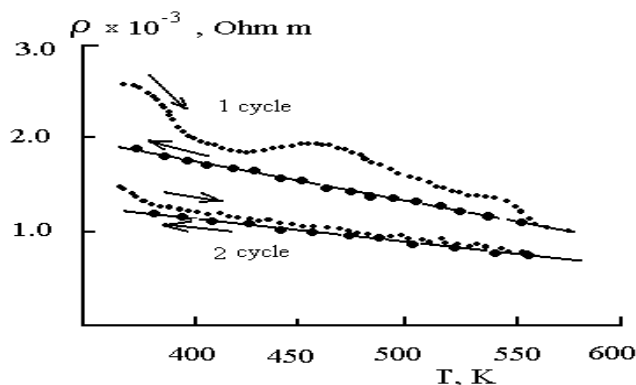


Figure 6. Dependence of resistivity of the $\text{Ge}_{1-x}\text{Si}_x$ ($x=0.15$) solid solution versus temperature: (1) before irradiation, (2) after irradiation.

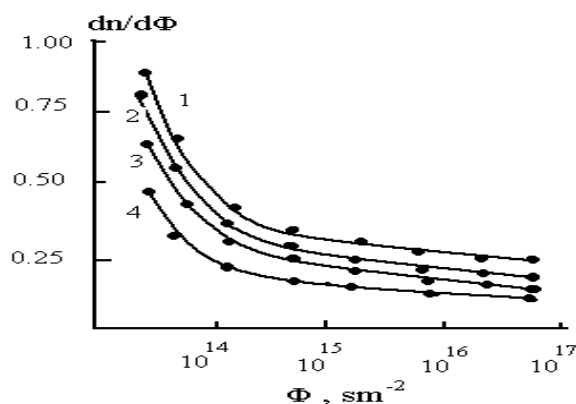


Figure 7. Dependence of the rate of generation of defects versus the irradiation dose for various Si contents in $n\text{-Ge}_{1-x}\text{Si}_x$ solid solution: (1) $x=0$, (2) $x=0.05$, (3) $x=0.10$, (4) $x=0.15$.

It was established that the rate of formation of radiation-induced defects increases with the Si content in the n -type $\text{Ge}_{1-x}\text{Si}_x$ thin films (Figure 7), and the dose necessary to produce the n to p

conversion decreases. The higher the silicon content in the $\text{Ge}_{1-x}\text{Si}_x$ samples irradiated with the same relative doses of electrons, the higher the hole concentration after conversion of the conductivity type. The data obtained during the experiments concerning the action of accelerated electron fluxes on the mechanical properties of the $\text{Ge}_{1-x}\text{Si}_x$ crystals can be explained if we suppose that the simplest defects in the crystal structure induced by the irradiation are vacancy-type lattice defects [16].

4. CONCLUSION

The Ge–Si solid solution is an inhomogeneous material, and it can be considered as a two-phase system. The interface between the phases is a source of strong elastic strains and is characterized by the maximum density of dislocations. Taking into account these considerations, we proposed a model to explain the radiation effects in $\text{Ge}_{1-x}\text{Si}_x$ involving the concept of structure inhomogeneity of the solid solutions consisting of the regions enriched with Si or Ge. The interface between these regions acts as an effective drain for interstitial atoms formed owing to the irradiation. The intensive adsorption and the accumulation of free vacancies in bulk define the peculiarities of the radiation processes in $\text{Ge}_{1-x}\text{Si}_x$ solid solutions and devices on their basis. According to the proposed model, the point defects formed in $\text{Ge}_{1-x}\text{Si}_x$ interact with structural defects and form complexes that act as recombination centers and decrease the concentration of charge carriers. This results in changes in the mechanical and electrical characteristics of the irradiated samples.

References

1. T.M. Razykov, C.S. Ferekides, D. Morel, E. Stefanakos, H.S. Ullal and H.M. Upadhyaya, *Solar Energy* 85 (2011) 1580
2. Sh.M. Abbasov, *Silicon Solid Solutions*, Baku, Elm. 2003.
3. R.A. Smith, *Semiconductors*, Cambridge University Press, 1961.
4. G.Kh. Adzharov, A.S. Ganiev and M.G. Shakhtakhtinski, *Dokl. AN Azerb. SSR*, 37 (1981) 36.
5. Sh.M. Abbasov, V.S. Mamedov, V.I. Shakhovtsov, G.M. Gasumov and L.I. Zagainova, *Dokl. AN Azerb. SSR*, 36 (1980) 33.
6. L. Wang, D. Hou, j. yu and w. wei, *Current Applied Physics*, 13 (2013) 688.
7. N.A. Agaev and G.Kh. Adzharov, *Mater. Dokl. Baku*, (1990) 56.
8. L.S. Palatnik` and Papirov, *Oriented Crystallization*, M. Metallurgiya, 1967.
9. S. Sakiyama, T. Kaneko, T. Ootsubo, T. Sakai and I. Tsunoda, *Thin Solid Films*, 11 (2013) 4.
10. L.S. Palatnik, M.Y. Fuks and V.M. Kosevich, *Mechanism of Formation and Substructure of Condensed Films*, M. Nauka, 1972.
11. B. T. Goh, S. K. Ngoi and S. A. Rahman, *Journal of Non-Crystalline Solids*, 363 (2013) 13.
12. S. J. Yun, J. K. Kim, S. H. Lee and Y. J. Lee, *Thin Solid Films*, 546 (2013) 362.
13. B. T. Goh, S. K. Ngoi, S. L. Yap and S. A. Rahman, *Thin Solid Films*, 529 (2013) 159.
14. A.S. Baytsar, Sh.M. Abbasov and Z.A. Ibrahimov, *Baku journal fizika*, XIII 5 (2007) 11.
15. Sh. M. Abbasov, G. T. Agaverdiieva, A. S. Baitsar, U. F. Faradzhova and G. M. Mekhdevi, *SURFACE ENG. and A. ELECTROCHEMISTRY*, 45 (2009) 161.
16. G. T. Agaverdiieva, Sh. M. Abbasov and H. Mahdavi, *Semiconductor Physics, Quantum Electronics & Optoelectronics*, 12 (2009) 357.